Supporting Information

Slow relaxation dynamics of a mononuclear Er(III) complex surrounded by a ligand environment with anisotropic charge density

Kwang Soo Lim,[a] Dong Won Kang,[a] Jeong Hwa Song,[a] Han Geul Lee,[a] Mino Yang,[b] and Chang Seop Hong*[a]

[a] *Department of Chemistry, Korea University, Seoul 136-713, Republic of Korea*
[b] *Space-Time Resolved Molecular Imaging Research Team, Korea Basic Science Institute, Seoul 136-713, Korea*

Table S1. Crystallographic Details of **1** - **4** and diluted-**2**.

	1	**2**	diluted-**2**	**3**	**4**
formula	$C_{22}H_{50}Co_2ErF_6O_{20}P_7$	$C_{22}H_{46}Co_2ErNO_{21}P_6$	$C_{22}H_{46}Co_2Y_{0.94}Er_{0.06}NO_{21}P_6$	$C_{22}H_{50}Co_2GdF_6O_{20}P_7$	$C_{22}H_{46}Co_2GdNO_{21}P_6$
Mr	1250.53	1131.54	1057.89	1240.52	1121.53
T (K)	296(2)	296(2)	296(2)	296(2)	296(2)
crystal system	orthorhombic	monoclinic	monoclinic	orthorhombic	monoclinic
space group	P2(1)2(1)2	P2(1)/c	P2(1)/c	P2(1)2(1)2	P2(1)/c
a (Å)	11.091(6)	12.2730(5)	12.3602(7)	11.1145(2)	12.4201(2)
b (Å)	21.203(12)	19.4424(7)	19.5310(11)	21.3469(3)	19.5445(4)
c (Å)	9.340(5)	16.7578(6)	16.8377(9)	9.32870(10)	16.8392(3)
α (°)	90	90	90	90	90
β (°)	90	102.974(2)	102.868(3)	90	102.4585(8)
γ (°)	90	90	90	90	90
V (Å^3)	2196(2)	3896.6(3)	3962.7(4)	2213.33(6)	3991.37(13)
Z	2	4	4	2	4
ρ_{calc} (g cm^{-3})	1.891	1.929	1.773	1.861	1.866
μ (mm^{-1})	2.990	3.302	2.639	2.569	2.782
F(000)	1246	2260	2151	1238	2244
total reflections	5119	9789	9894	5502	9912
GOF	0.634	0.941	1.048	1.046.	1.035
R1[a] (I≥2σ(I))	0.0322	0.0607	0.0357	0.0302	0.0242
wR2[b] (I≥2σ(I))	0.0798	0.1207	0.0830	0.0715	0.0577

[a] $R1=\Sigma||F_O|-|F_C||/\Sigma|F_C|$, [b] $wR2 = [\Sigma w(F_O^2 - F_C^2)^2/\Sigma w(F_O^2)^2]^{1/2}$

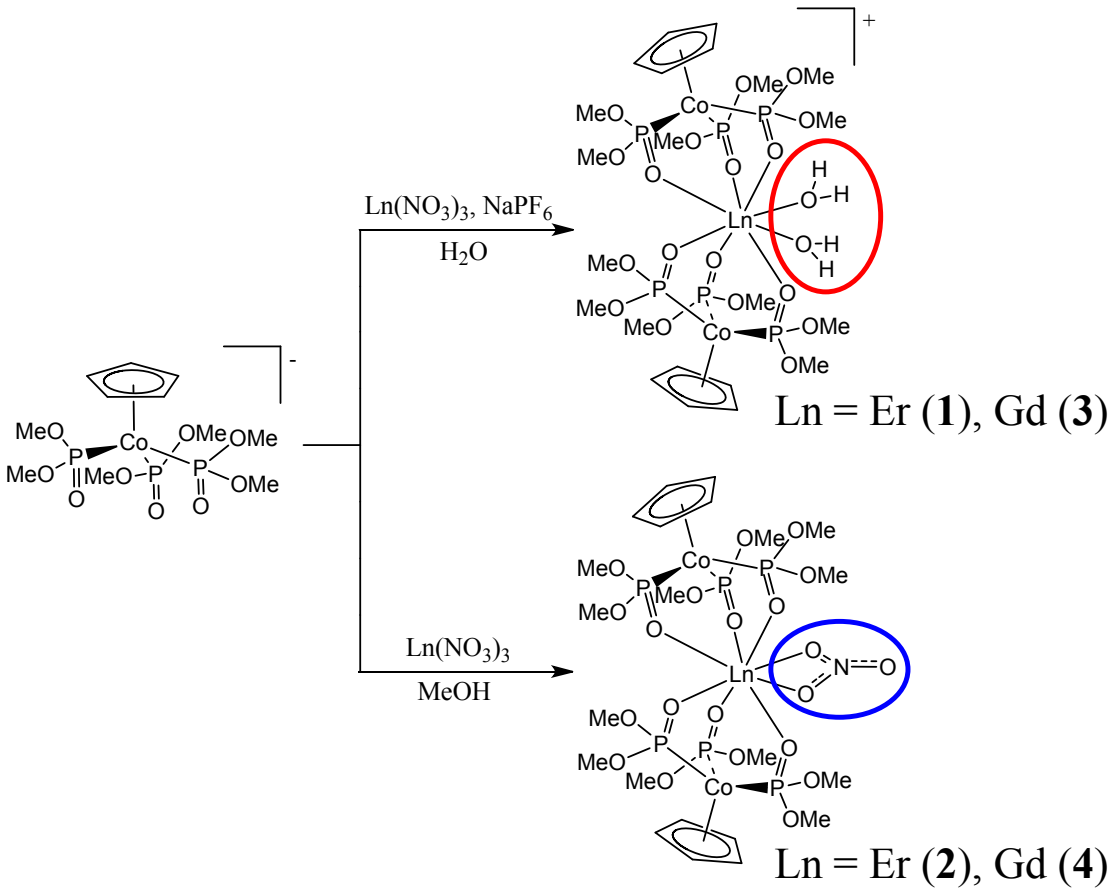

Scheme S1. Synthetic procedure for **1**, **2**, **3** and **4**.

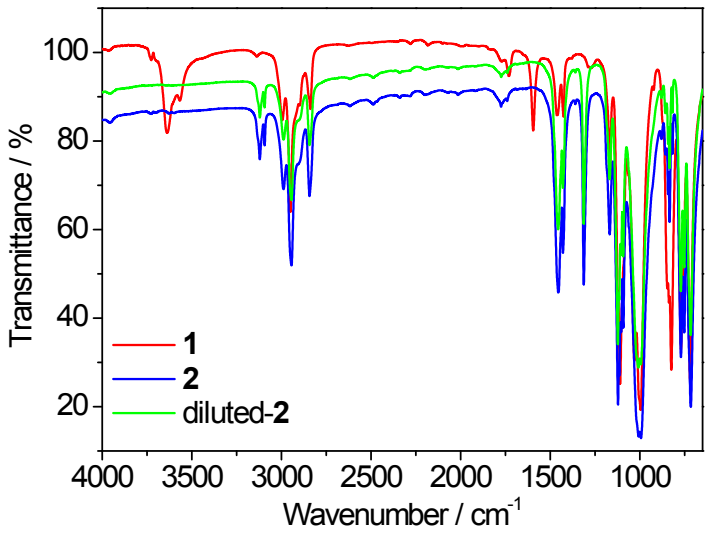

Fig. S1 IR spectra of **1**, **2**, and **diluted-2**.

Table S2. Selected Bond Distances (Å)

1			
Dy1-O1	2.2825(1)	Dy1-O2	2.3328(1)
Dy1-O3	2.3714(1)	Dy1-O10	2.4881(1)
2			
Dy1-O1	2.3400(1)	Dy1-O2	2.3253(1)
Dy1-O3	2.2887(1)	Dy1-O4	2.2893(1)
Dy1-O5	2.3271(1)	Dy1-O6	2.3314(1)
Dy1-O19	2.5075(1)	Dy1-O20	2.4933(1)
diluted-**2**			
Y1,Er1-O1	2.3372(1)	Y1,Er1-O2	2.3156(1)
Y1,Er1-O3	2.2867(1)	Y1,Er1-O4	2.2828(1)
Y1,Er1-O5	2.3187(1)	Y1,Er1-O6	2.3374(1)
Y1,Er1-O19	2.5031(1)	Y1,Er1-O20	2.4867(1)
3			
Gd1-O1	2.3185(0)	Gd1-O2	2.3548(0)
Gd1-O3	2.3977(0)	Gd1-O10	2.5095(0)
4			
Gd1-O1	2.3731(0)	Gd1-O2	2.3534(0)
Gd1-O3	2.3265(0)	Gd1-O4	2.3238(0)
Gd1-O5	2.3589(0)	Gd1-O6	2.3735(0)
Gd1-O19	2.5390(0)	Gd1-O20	2.5306(0)

Table S3. Results of the continuous shape measure analysis.

Metal center	Shape Measures(S_X) relative to SAPR-8	DD-8
Er1 (**1**)	0.821	1.181
Er1 (**2**)	1.283	2.429
Y, Er1 (diluted-**2**)	1.300	2.499
Gd1 (**3**)	0.930	1.054
Gd1 (**4**)	1.299	2.611

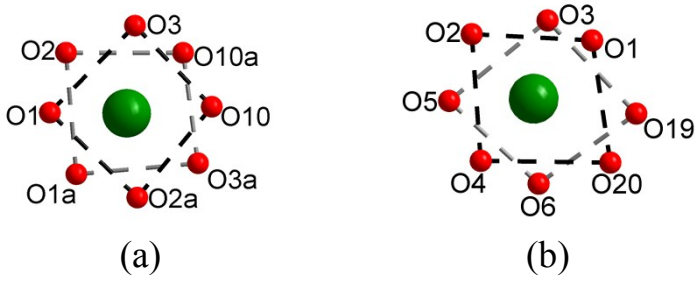

Fig. S2 Coordination symmetry of (a) **1** and (b) **2**.

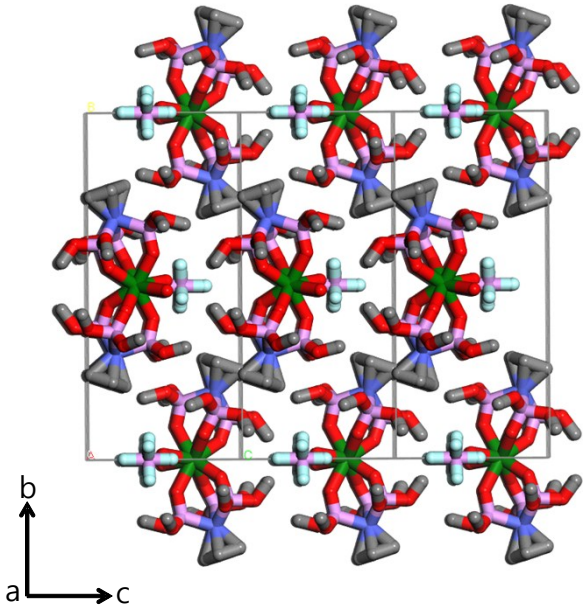

Fig. S3 Packing diagram of **1**.

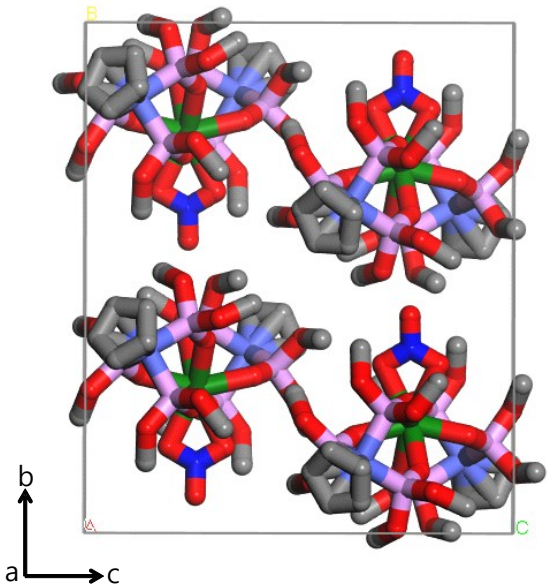

Fig. S4 Packing diagram of **2**.

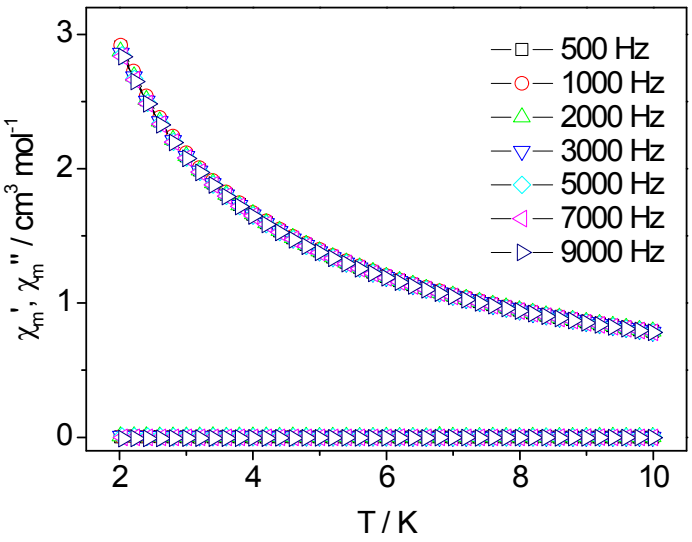

Fig. S5 Temperature-dependent ac magnetic susceptibility data of **1** at zero dc field.

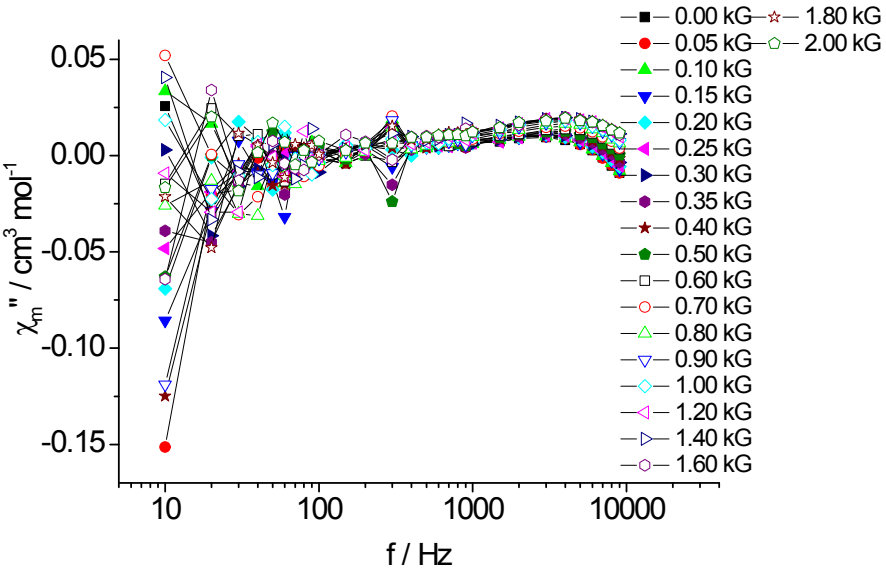

Fig. S6 Field-dependent ac magnetic susceptibilities of **1**.

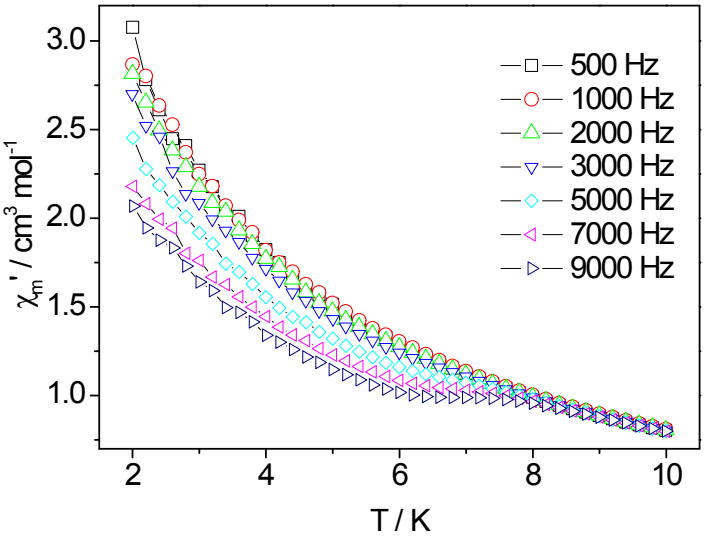

Fig. S7 Plot of in-phase signals versus T for **2** at zero dc field.

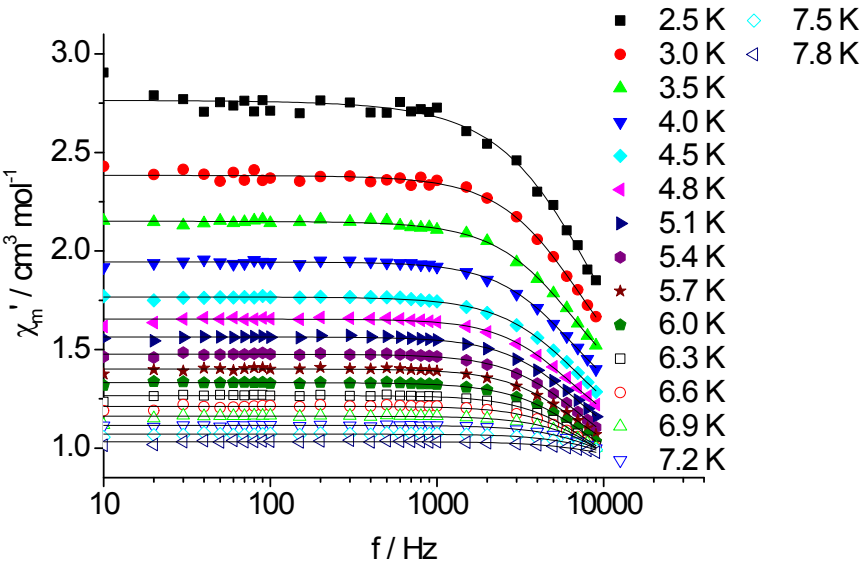

Fig. S8 Plot of out-of-phase signals versus *f* for **2** at zero dc field.

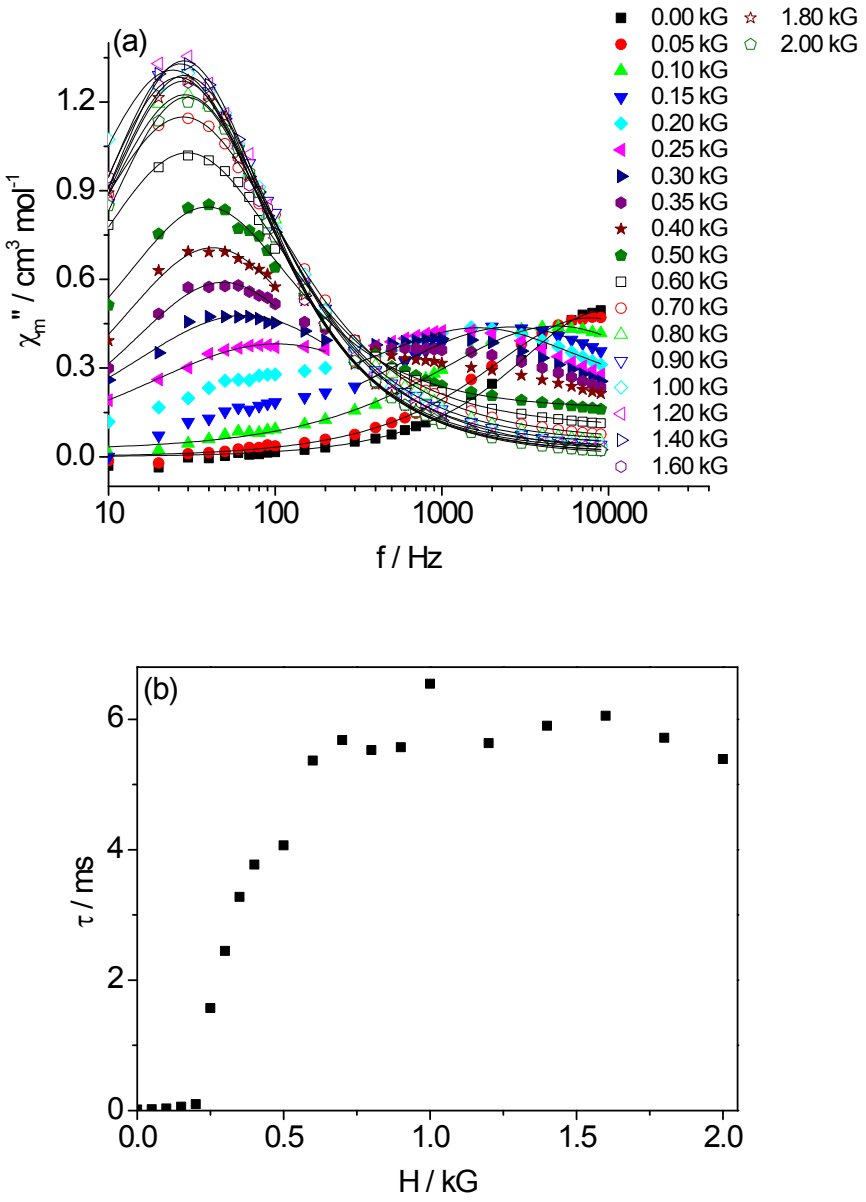

Fig. S9 (a) Plot of out-of-phase signals versus *f* for **2** at an ac field of 3 G, T = 4 K and several dc fields. The solid lines are best fits to the generalized Debye model. (b) Plot of the relaxation time (τ) as a function of applied dc magnetic field at 4 K for **2**.

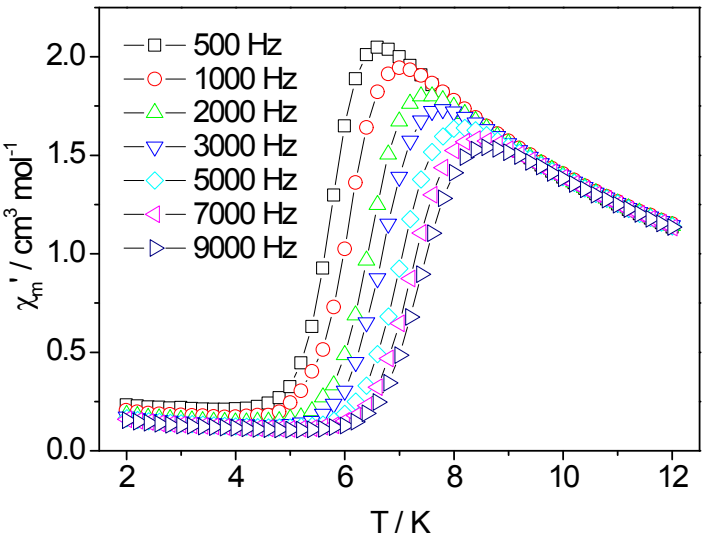

Fig. S10 Plot of in-phase signals versus T for **2** at H_{dc} = 1.0 kG.

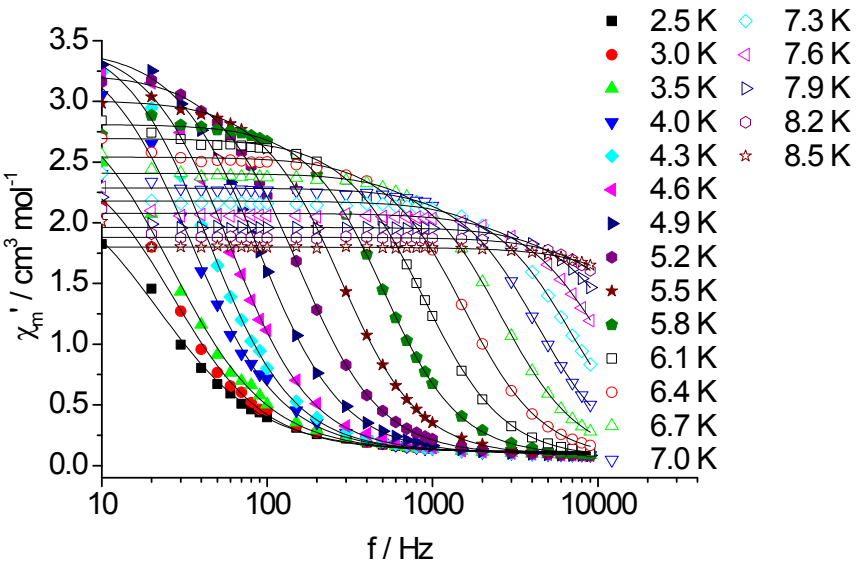

Fig. S11 Plot of out-of-phase signals versus *f* for **2** at H_{dc} = 1.0 kG.

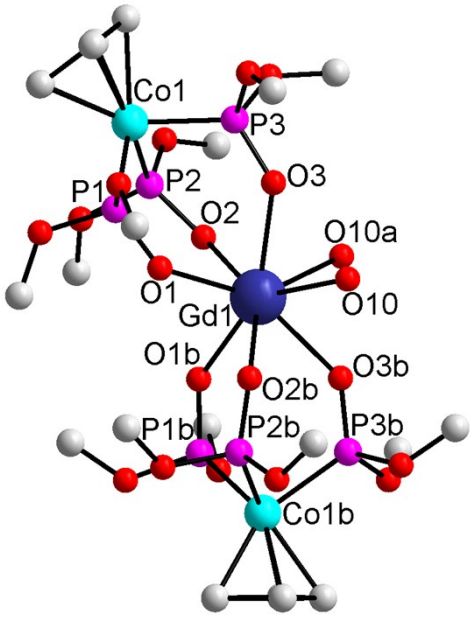

(a)

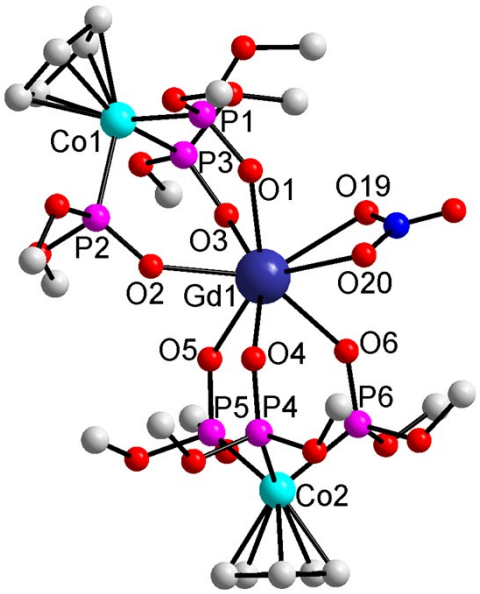

(b)

Fig. S12 (a) Molecular structure of the cationic part of **3**. Symmetry code: b = 1-x, -y, z. (b) Molecular view of **4**.

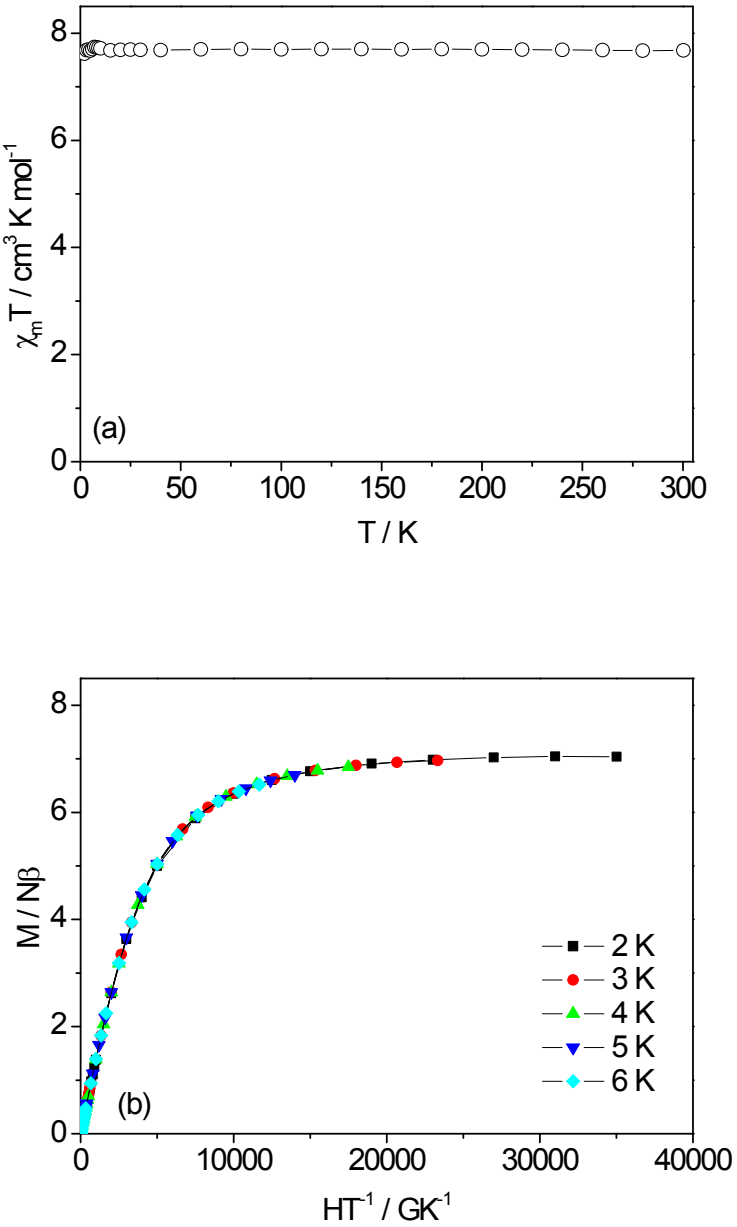

Fig. S13 (a) Plot of $\chi_m T$ versus T of **3** from 2 to 300 K. (b) Plot of M versus H/T at the indicated temperatures.

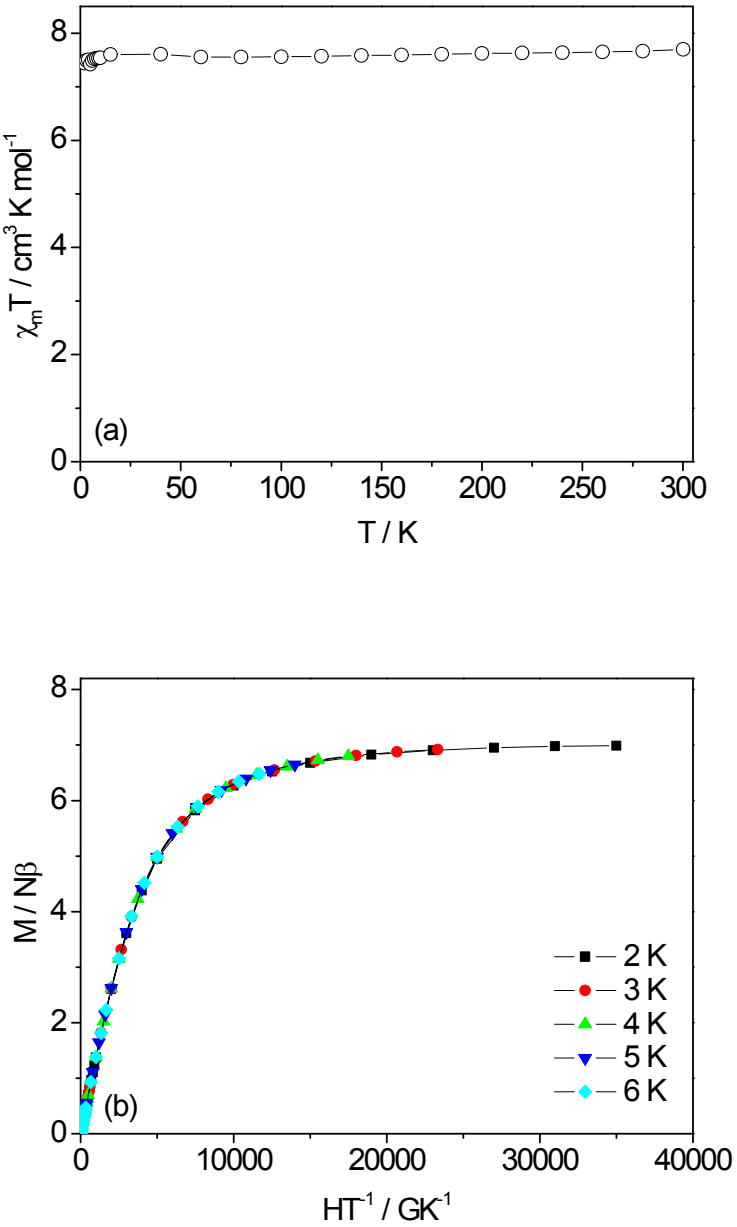

Fig. S14 (a) Plot of $\chi_m T$ versus T of **4** from 2 to 300 K. (b) Plot of M versus H/T at the indicated temperatures.

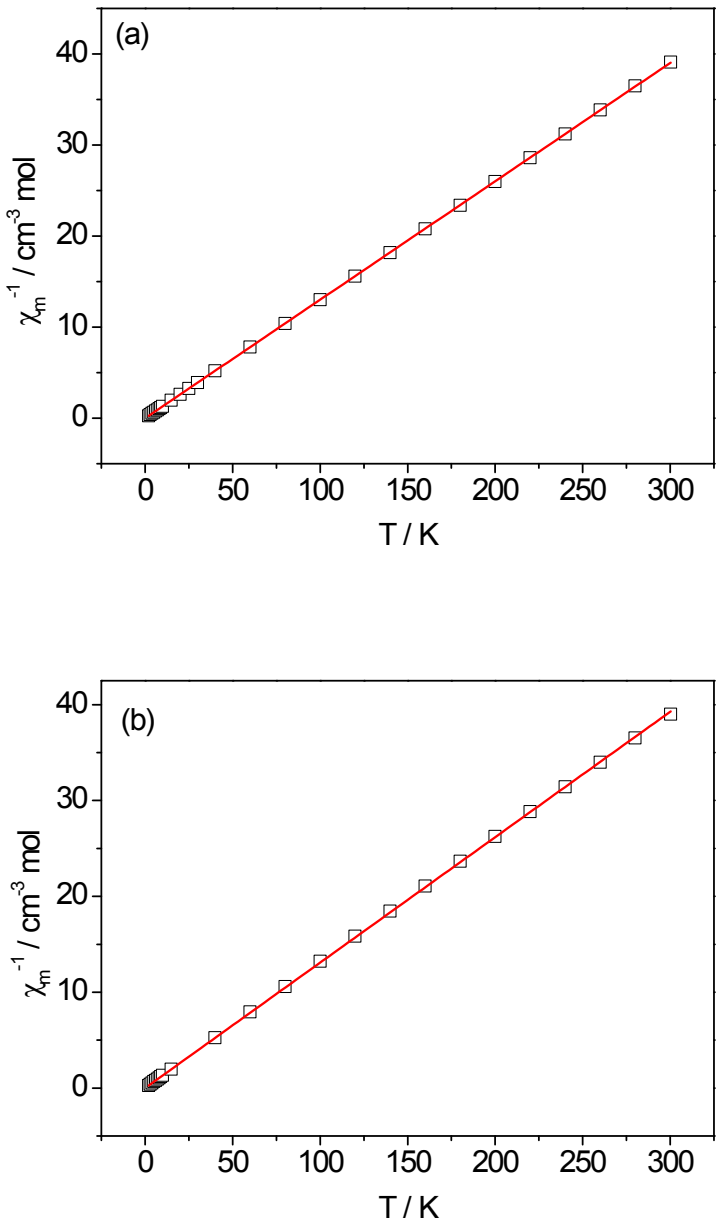

Fig. S15 Plots of $1/\chi_m$ versus T of **3** (a) and **4** (b). The solid line is best fit to the Curie-Weiss law.

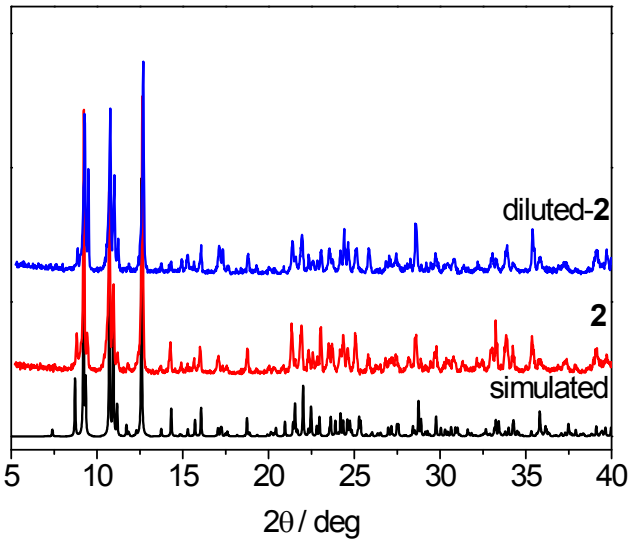

Fig. S16 PXRD data for **2** and **diluted-2**.

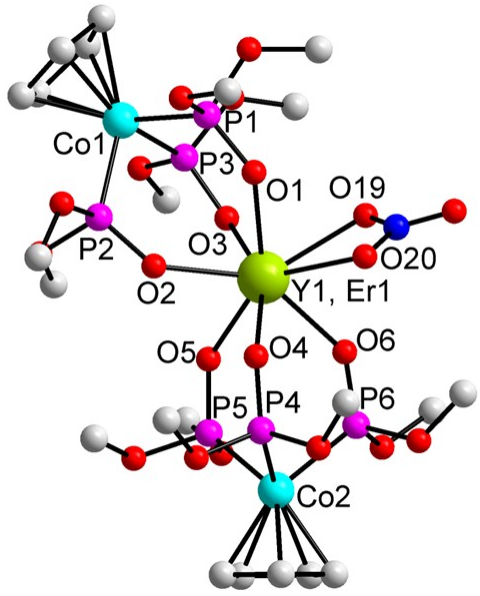

Fig. S17 Crystal structure of **diluted-2**.

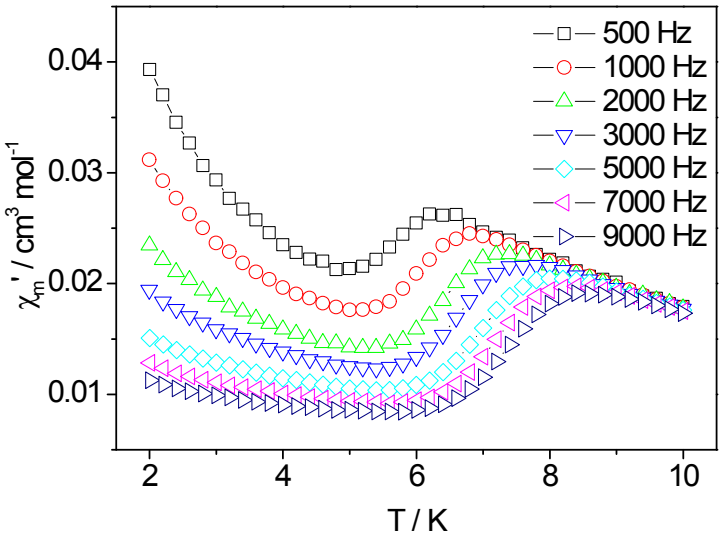

Fig. S18 Plot of in-phase signals versus T for **diluted-2** at zero dc field.

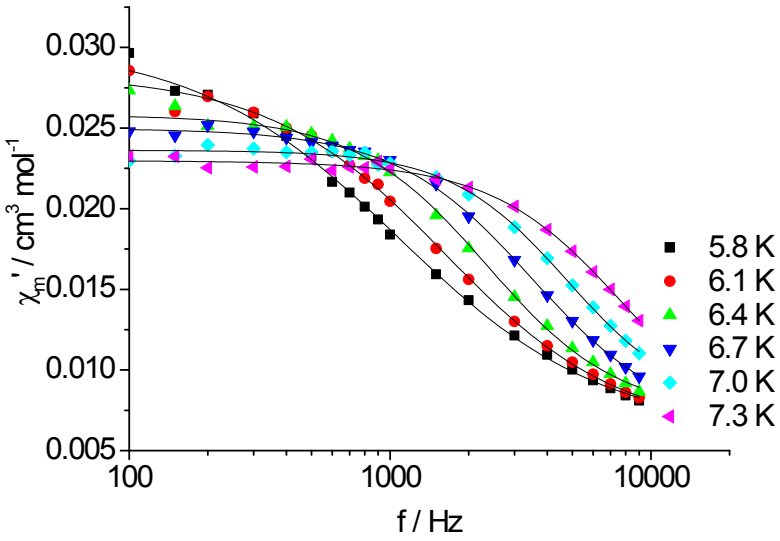

Fig. S19 Plot of out-of-phase signals versus *f* for **diluted-2** at zero dc field.

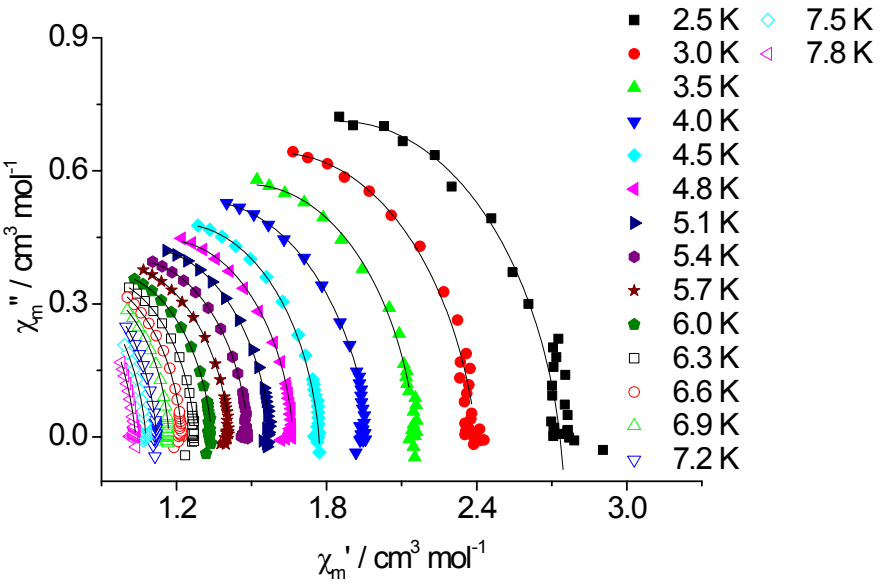

Fig. S20 Cole-Cole plots for **2** at zero external field. The solid lines indicate theoretical tits of the data.

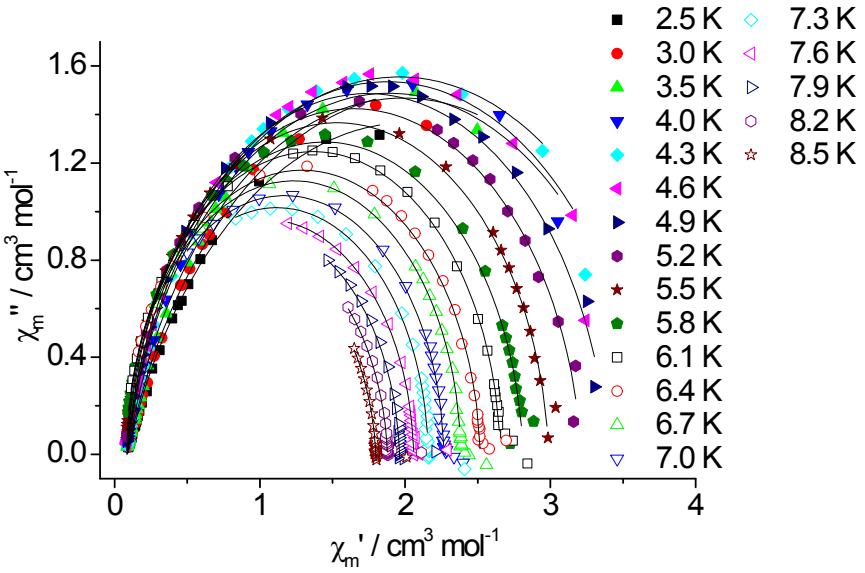

Fig. S21 Cole-Cole plots for **2** at H_{dc} = 1.0 kG. The solid lines indicate theoretical tits of the data.

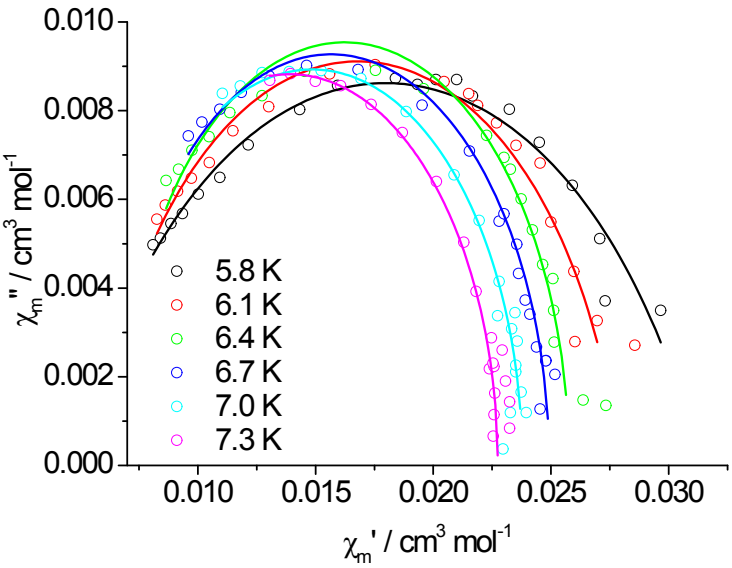

Fig. S22 Cole-Cole plots for diluted-**2** at zero external field. The solid lines indicate theoretical tits of the data.

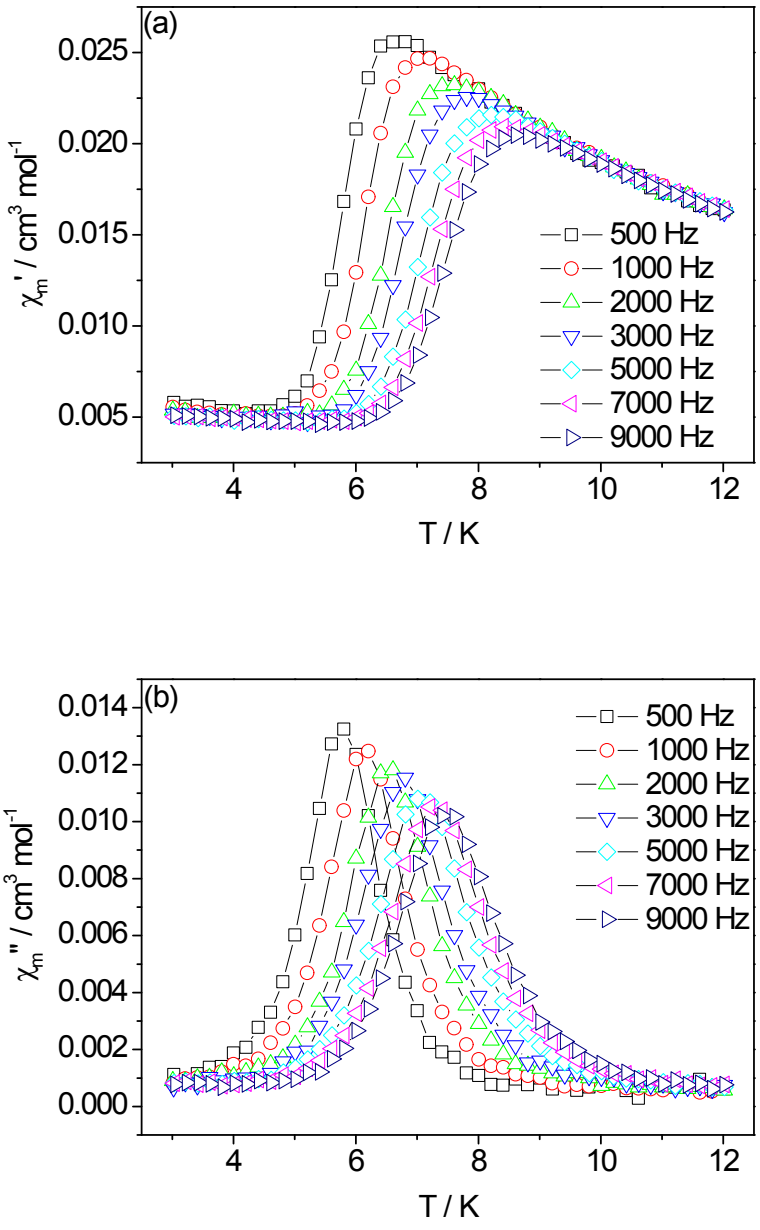

Fig. S23 Plot of in-phase (a) and out-of-phase signals (b) versus *T* for **diluted-2** at H_{dc} = 1.0 kG.